Revista de metalurgia

# Kinetics of the electrolytic $Fe^{2+}/Fe^{3+}$ oxidation on various anode materials(•)

L. Cifuentes* and R. Glasner*

**Abstract** The kinetics of the electrolytic $Fe^{2+}/Fe^{3+}$ oxidation, relevant to hydro-electrometallurgical processing, have been studied on lead, platinum, ruthenium oxide, iridium oxide and graphite anodes in ferrous sulfate-sulfuric acid solutions. The oxidation rate depends on ferrous sulfate concentration, solution temperature and degree of agitation. Potentiodynamic studies show that: a) the highest oxidation rate is obtained on platinum; b) lead is unsuitable as anodic material for the said reaction; c) the remaining anode materials show a similar and satisfactory performance.

**Keywords** Anode. Kinetics. Ferrous ion. Oxidation.

## Cinética de la oxidación electrolítica $Fe^{2+}/Fe^{3+}$ sobre varios materiales anódicos

**Resumen** Se ha estudiado la cinética de la oxidación electrolítica $Fe^{2+}/Fe^{3+}$ -relevante para el procesamiento hidroelectrometalúrgico- sobre plomo, platino, óxido de rutenio, óxido de iridio y grafito en soluciones de sulfato ferroso en ácido sulfúrico. La velocidad de oxidación depende de la concentración de sulfato ferroso, la temperatura de la solución y el grado de agitación. Estudios potenciodinámicos demuestran que: a) las mayores velocidades de oxidación se obtienen sobre platino; b) el plomo es inadecuado como material anódico para la reacción mencionada; c) los materiales anódicos restantes exhiben un desempeño similar y satisfactorio.

**Palabras clave** Ánodo. Cinética. Ion ferroso. Oxidación.

## 1. INTRODUCTION

### 1.1. Objective

This work aims to study the effectiveness of various anode materials to sustain the electrolytic $Fe^{2+}/Fe^{3+}$ oxidation in ferrous sulfate - sulfuric acid solutions. This reaction is relevant to hydro-electrometallurgical processing and its study was motivated by the development of a new copper electrowinning cell which uses ferrous ion oxidation as anodic reaction[1].

### 1.2. Previous work

The limitations of conventional copper electrowinning cells have been discussed by several authors[2-12]. One of these limitations is the high energy requirement (about 2 kWh per kg of produced copper), which is a result of an anodic reaction ($2\ H_2O \rightarrow O_2 + 4\ H^+ + 4e$) which takes place on a lead alloy. The standard equilibrium potential for this reaction is 0.89 V higher than the corresponding value for the cathodic reaction ($Cu^{2+} + 2e \rightarrow Cu^0$); it also exhibits an anodic overpotential close to 0.8 V. Additionally, this reaction produces 'acid mist' (air contamination with sulfuric acid) in industrial plants

Dew and others[5, 6, 13 and 14] have studied the substitution of an energetically advantageous anodic reaction. Several such reactions have been considered[5 and 7], but some of them involve toxic reactants or products while others require expensive chemicals. A less problematic reaction, which has produced cell voltage reductions, is $Fe^{2+} \rightarrow Fe^{3+} + e$. It exhibits a standard equilibrium potential 0.46 V lower than that of the conventional water decomposition reaction. In addition, depending on the nature of the anode material, it may also produce lower anodic overpotentials. An added benefit from the $Fe^{2+}/Fe^{3+}$ oxidation is that ferric ion can be used as an oxidizing agent in combined leaching processes; it may also produce ferric compounds of

(•) Trabajo recibido el día 21 de abril de 2003 y aceptado en su forma final el día 6 de junio de 2003.
(*) Departamento de Ingeniería de Minas, Universidad de Chile, Tupper 2069, Santiago, Chile.

commercial value. Lab and pilot plant scale tests have shown that the cell voltage can be reduced from 2 V (typical of conventional copper electrowinning cells) to about 1 V [14] when anolyte and catholyte are kept separate by an appropriate membrane. Without such separation, the presence of ferric ion has resulted in a drastic decrease of the cathodic current efficiency due to ferric to ferrous ion reduction on the cathode.

Materials other than lead have been proposed as anodes: precious metal oxide coatings[5 and 14], coke[15] and mixtures of Ir, Sb and Sn oxides[16]. Other authors have studied the $Fe^{2+}/Fe^{3+}$ oxidation[17-23] and phenomena relevant to the electrocatalysis and electrochemical behaviour of anodes made of lead and other materials[24-30]. The ferrous to ferric oxidation reaction was used in a 'spouted bed' electrowinning cell[15], but the resulting current efficiency was unsatisfactory.

## 2. EXPERIMENTAL

A Solartron 1286 electrochemical interface was used to perform potentiodynamic experiments in order to characterize the kinetics of the electrolytic $Fe^{2+}/Fe^{3+}$ oxidation on various materials: lead sheet (Pb), platinum sheet (Pt), platinum on titanium mesh (Pt/Ti), ruthenium bioxide on titanium mesh ($RuO_2$/Ti), iridium bioxide on titanium mesh ($IrO_2$/Ti) and graphite.

A three-electrode glass cell with double jacket was used in order to keep the temperature constant at 25 or 50 °C. The working electrode was the material to be studied. The counter electrode was made of platinum and its surface area was 10 $cm^2$.The reference electrode was $Hg/HgSO_4$ (0.648 V vs. SHE at 25 °C and 0.645 V at 50 °C). The sweep rate was 0.5 mV/s. Electrolytes were agitated by means of a Nova II magnetic agitator.

The tested variables were: concentration of anolyte (aqueous $FeSO_4$ + $H_2SO_4$) and catholyte (aqueous $CuSO_4$ + $H_2SO_4$), electrolyte temperature and degree of agitation. Conditions are presented in table I. Agitation refers to the setting on the Nova II magnetic agitator; setting 2 = 185 rpm; setting 7 = 510 rpm; dimensions of stir bar: 50 mm length, 9 mm diameter; mass = 15.1 g. The temperature was controlled, in all cases, by means of a Julabo thermostatic bath. Analytical purity chemicals were used to prepare the synthetic electrolytes.

Exchange current densities, limiting current densities and charge transfer coefficients were obtained by fitting appropriate equations (see below) to experimental results.

**Table I.** Experimental conditions for potentiodynamic experiments

*Tabla I. Condiciones experimentales para experimentos potenciodinámicos*

| Condition | $[H_2SO_4]$ M | $[FeSO_4]$ M | Agitation setting[a] | Temperature °C |
|---|---|---|---|---|
| 1 | 0.05 | 0.5 | 2 | 25 |
| 2 | 0.5 | 0.5 | 2 | 25 |
| 3 | 0.5 | 1.0 | 2 | 25 |
| 4 | 0.5 | 1.0 | 7 | 25 |
| 5 | 0.5 | 1.0 | 7 | 50 |

[a] Nova II agitator setting.
setting 2 = 185 rpm
setting 7 = 510 rpm
stir bar: 50 mm length, 9 mm diameter, mass = 15.1 g

[a] Posición en agitador Nova II.
posición 2 = 185 rpm
posición 7 = 510 rpm
agitador: 50 mm de largo, 9 mm de diámetro, masa = 15.1 g

The design of mesh anodes (Pt/Ti, $RuO_2$/Ti, $IrO_2$/Ti) is shown in figure 1. The graphite electrode was a solid cylinder, while the lead and platinum electrodes were in sheet form. The apparent anode surface area was 10 $cm^2$ in all cases.

A Tencor 500 Surface Profilometer with Alpha-Step software was used to determine the effective anode surface areas. Their values are in table II.

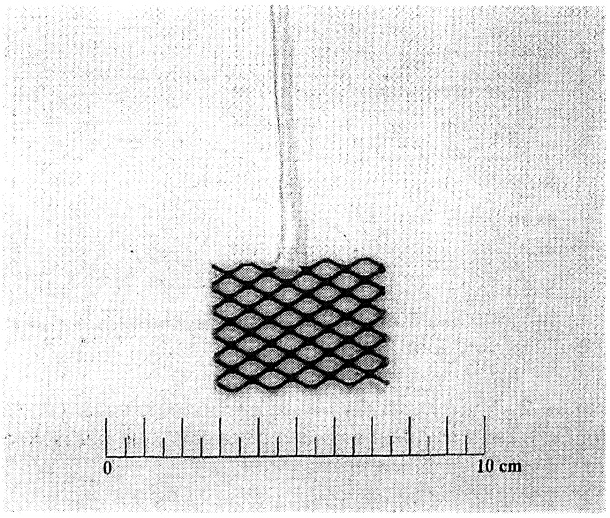


**Figure 1.** Mesh electrodes.

*Figura 1. Electrodos de malla.*

**Table II.** Effective anode surface areas

*Tabla II. Áreas superficiales efectivas de ánodos*

| Apparent anode | Effective surface area, $cm^2$ |
|---|---|
| | 10 |
| Anode material | |
| Platinum sheet | 10.0 |
| Lead sheet | 10.0 |
| Graphite cylinder | 12.6 |
| Pt/Ti mesh | 14.6 |
| $RuO_2$/Ti mesh | 12.1 |
| $IrO_2$/Ti mesh | 15.4 |

## 3. RESULTS

Figures 2 to 7 show the $Fe^{2+}/Fe^{3+}$ oxidation kinetics. There is one figure for each studied material (six in total) and the curves represent the five conditions presented in table I. All electrode potentials are given against SHE.

It is clear from figures 2 to 6 that the oxidation rate increases with ferrous sulfate concentration, degree of agitation and temperature. The studied agitation increase (from 185 to 510 rpm) and temperature increase (from 25 °C to 50 °C) appear to have more impact on the reaction rate than the studied ferrous sulfate concentration increase (from 0.5 M to 1.0 M). Not surprisingly, the highest oxidation rates were obtained at condition 5 (see Table I), which includes 510 rpm, 50 °C and 1.0 M $FeSO_4$.

Figure 7 shows that lead is inadequate as anode material for the studied reaction, as the reaction

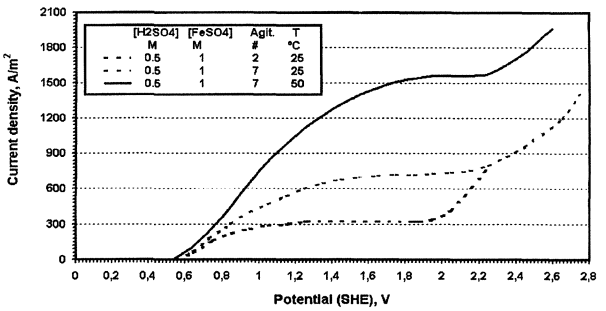


**Figure 2.** Current density versus electrode potential curves for $Fe^{2+}/Fe^{3+}$ oxidation on platinum anode. Agit = agitation setting on Nova II magnetic agitator.

*Figura 2. Curvas densidad de corriente versus potencial de electrodo para la oxidación $Fe^{2+}/Fe^{3+}$ sobre ánodo de platino. Agit = posición en la escala de agitación del agitador magnético Nova II.*

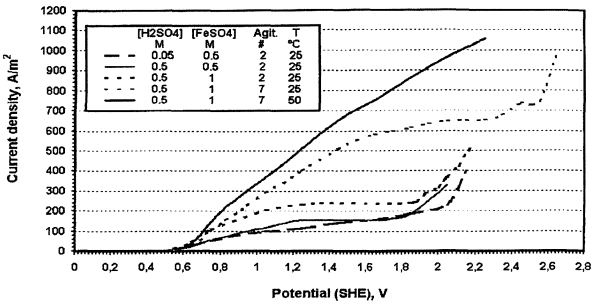


**Figure 3.** Current density versus electrode potential curves for $Fe^{2+}/Fe^{3+}$ oxidation on Pt/Ti anode. Agit = agitation setting on Nova II magnetic agitator.

*Figura 3. Curvas densidad de corriente versus potencial de electrodo para la oxidación $Fe^{2+}/Fe^{3+}$ sobre ánodo de Pt/Ti. Agit = posición en la escala de agitación del agitador magnético Nova II.*

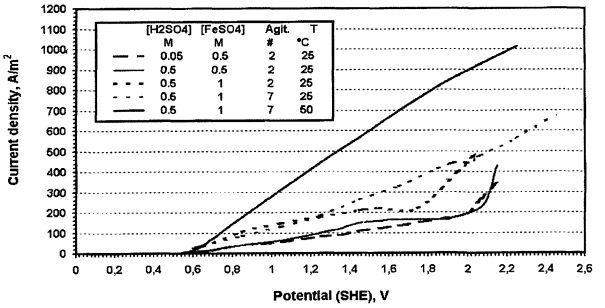


**Figure 4.** Current density versus electrode potential curves for $Fe^{2+}/Fe^{3+}$ oxidation on $IrO_2$/Ti anode. Agit = agitation setting on Nova II magnetic agitator.

*Figura 4. Curvas densidad de corriente versus potencial de electrodo para la oxidación $Fe^{2+}/Fe^{3+}$ sobre ánodo de $IrO_2$/Ti. Agit = posición en la escala de agitación del agitador magnético Nova II.*

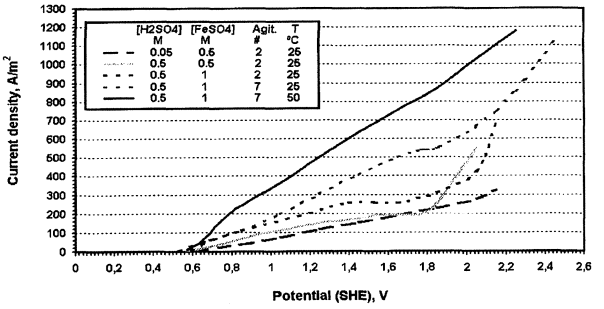


**Figure 5.** Current density versus electrode potential curves for $Fe^{2+}/Fe^{3+}$ oxidation on $RuO_2$/Ti anode. Agit = agitation setting on Nova II magnetic agitator.

*Figura 5. Curvas densidad de corriente versus potencial de electrodo para la oxidación $Fe^{2+}/Fe^{3+}$ sobre ánodo de $RuO_2$/Ti. Agit = posición en la escala de agitación del agitador magnético Nova II.*

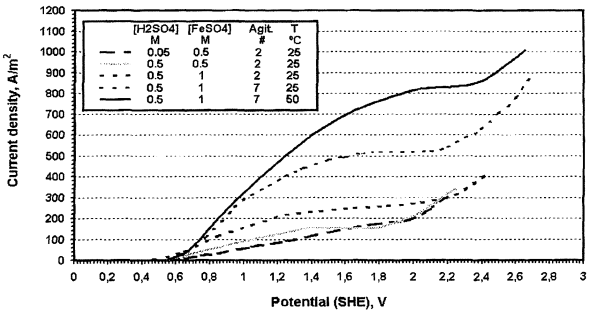


**Figure 6.** Current density versus electrode potential curves for $Fe^{2+}/Fe^{3+}$ oxidation on graphite anode. Agit = agitation setting on Nova II magnetic agitator.

*Figura 6. Curvas densidad de corriente versus potencial de electrodo para la oxidación $Fe^{2+}/Fe^{3+}$ sobre ánodo de grafito. Agit = posición en la escala de agitación del agitador magnético Nova II.*

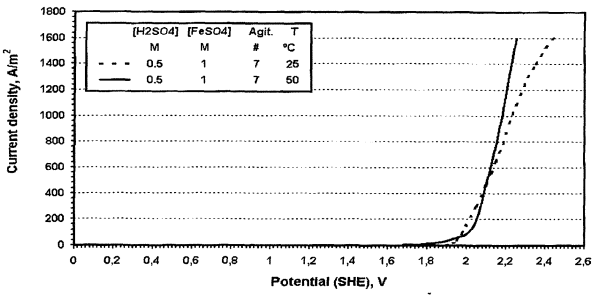


**Figure 7.** Current density versus electrode potential curves for $Fe^{2+}/Fe^{3+}$ oxidation on Lead anode. Agit = agitation setting on Nova II magnetic agitator

*Figura 7. Curvas densidad de corriente versus potencial de electrodo para la oxidación $Fe^{2+}/Fe^{3+}$ sobre ánodo de plomo. Agit = posición en la escala de agitación del agitador magnético Nova II.*

rate is practically negligible throughout the relevant potential range. On the other hand, the curve shows that lead is a good catalyst for anodic decomposition of water.

The data in figures 2 to 7 also allow comparison of the kinetics on various anodes for each one of the studied conditions. As an example, figure 8 depicts the kinetics of ferrous to ferric ion oxidation at condition 5 on Pt, Pb, Pt/Ti, $IrO_2$/Ti, $RuO_2$/Ti and graphite. It can be concluded that the highest oxidation rates are achieved on Pt sheet and the lowest, on Pb sheet. Figure 8 also makes it clear that the reaction rates on the remaining four materials are remarkably similar.

Values for $i_L$, $i_o$ and $\alpha_a$ were determined from the above curves. To this end, experimental results were used to fit mixed-control equations using Excel Solver software. The equations were derived

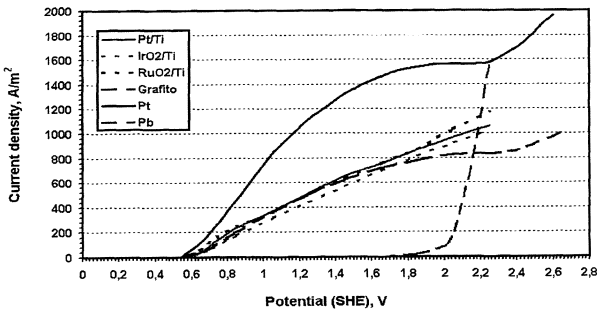


**Figure 8.** Current density versus electrode potential curves for $Fe^{2+}/Fe^{3+}$ oxidation on various anode materials at condition 5 ($[H_2SO_4]$ = 0.5 M, $[FeSO_4]$ = 1.0 M, T = 50 °C and agitator setting = 7).

*Figura 8. Curvas densidad de corriente versus potencial para la oxidación $Fe^{2+}/Fe^{3+}$ sobre varios materiales anódicos en la condición 5 ($[H_2SO_4]$ = 0.5 M, $[FeSO_4]$ = 1.0 M, T = 50°C y posición de agitador = 7).*

from Fick's law for mass transfer control, Butler-Volmer equation for charge transfer control and a relationship which links them both[12 and 31]:

$$\frac{1}{i_{MC}} = \frac{1}{i_{CTC}} + \frac{1}{i_{MTC}} \qquad (1)$$

The resulting expressions are, for an anodic reaction:

$$i_{MC} = \frac{i_{0,a} i_{L,a}}{i_{0,a} + i_{L,a} \exp\left(\frac{-\alpha_a F}{RT}\eta\right)} \qquad (2)$$

and, for a cathodic reaction:

$$|i_{MC}| = \frac{i_{0,c}|i_{L,c}|}{i_{0,c} + |i_{L,c}| \exp\left(\frac{\alpha_c F}{RT}\eta\right)} \qquad (3)$$

Table III gives the limiting current density for the electrolytic $Fe^{2+}/Fe^{3+}$ oxidation on each of five materials (lead was excluded) and for each of five conditions.

Table IV shows exchange current densities and charge transfer coefficients for ferrous ion oxidation on each of five materials (Pt, Pt/Ti, $RuO_2$/Ti, $IrO_2$/Ti and graphite) obtained at conditions 4 and 5 (see Table I), which produced the highest reaction rates. Calculation of these parameters requires knowledge of the equilibrium potential for the electrolytic $Fe^{2+}/Fe^{3+}$ oxidation. This was achieved by measuring the rest potential on a platinum electrode for the studied electrolytes

**Table III.** Limiting current densities (in A $m^{-2}$) for various anode materials and experimental conditions[a]

*Tabla III. Densidades de corriente límite (en A $m^{-2}$) para varios materiales anódicos y condiciones experimentales[a]*

| Condition | Pt | Pt/Ti | $IrO_2$/Ti | $RuO_2$/Ti | Graphite |
|---|---|---|---|---|---|
| 1 | - | NO[b] | NO | NO | 133 |
| 2 | - | 154 | 165 | 193 | 153 |
| 3 | 320 | 240 | 221 | 248 | 260 |
| 4 | 720 | 648 | 441 | 573 | 519 |
| 5 | 1560 | NO | NO | NO | 832 |

[a]Conditions are defined in table I.

[b]NO = not observed

[a]Las condiciones están definidas en la tabla I.

[b]NO = no se observa.

**Table IV.** Kinetic parameters for $Fe^{2+}/Fe^{3+}$ oxidation on various anode materials and two experimental conditions[a]

*Tabla IV. Parámetros cinéticos para la oxidación $Fe2^{+}/Fe^{3+}$ sobre varios materiales anódicos y dos condiciones experimentales[a]*

| Material | Condition 4 | | Condition 5 | |
|---|---|---|---|---|
| | $i_0$, A/$m^2$ | $\alpha_a$ | $i_0$, A/$m^2$ | $\alpha_a$ |
| Pt | 57.2 | 0.15 | 108.4 | 0.14 |
| Pt/Ti | 43.8 | 0.11 | 89.1 | 0.08 |
| $RuO_2$/Ti | 23.2 | 0.12 | 75.4 | 0.09 |
| $IrO_2$/Ti | 18.7 | 0.10 | 63.7 | 0.08 |
| Graphite | 31.4 | 0.15 | 51.2 | 0.12 |

[a]Conditions are defined in table I.

[a]Las condiciones están definidas en la tabla I.

at condition 4 (0.507 V) and condition 5 (0.501 V).

Table V shows calculated values for the overpotential of the anodic reaction at condition 5 with three applied current densities.

A ranking of the catalytic capacities of the studied anode materials can be obtained from these data.

## 4. DISCUSSION

### 4.1. Agitation

The $Fe^{2+}/Fe^{3+}$ oxidation rate increased with the degree of forced convection caused by mechanical agitation of the electrolyte. This is to be expected as the thickness of the diffusion layer ($\delta$), which forms next to the electrode surface, diminishes with increasing agitation, so that the limiting current density ($i_L$) increases according to Fick's law:

$$i_L = zFD\frac{c_{Fe^{2+}}}{\delta} = zFkc_{Fe^{2+}} \qquad (4)$$

Mesh electrodes (Pt/Ti, $RuO_2$/Ti, $IrO_2$/Ti) act as turbulence promoters, causing high levels of local mass transport, which, in turn, generate a marked increase in $i_L$ values (see Figs. 3, 4 and 5). These $i_L$ values are not reached before the onset of oxygen evolution, therefore the curves do not exhibit a plateau characteristic of mass transfer control. This seems to be confirmed by figures 2 (platinum sheet) and 6 (graphite rod). In these cases, where the electrodes are not in mesh form, a plateau is observed.

**Table V.** Overpotentials (in V) for $Fe^{2+}/Fe^{3+}$ oxidation at three applied current densities (condition 5[a])

*Tabla V. Sobrepotenciales (en V) para la oxidación $Fe^{2+}/Fe^{3+}$ a tres densidades de corriente aplicadas (condición 5[a])*

| $i_{cell}$, A/$m^2$ | 200 | 250 | 400 |
|---|---|---|---|
| Material | | | |
| Pt | 0.17 | 0.20 | 0.29 |
| Pt/Ti | 0.25 | 0.32 | 0.53 |
| $RuO_2$/Ti | 0.26 | 0.33 | 0.57 |
| $IrO_2$/Ti | 0.32 | 0.41 | 0.65 |
| graphite | 0.31 | 0.38 | 0.58 |

[a] Condition 5 is defined in table I.

[a] La condición 5 está definida en la tabla I.

### 4.2. Sulfuric acid concentration

Experiments performed with 0.05 M and 0.5 M sulfuric acid show that the effect of this variable on the electrolytic $Fe^{2+}/Fe^{3+}$ oxidation is very slight for all anode materials (Figs. 3, 4, 5 and 6). For 0.05M $H_2SO_4$ the anodic reaction, independently of anodic potential, does not show a mass transfer control range on mesh anodes (Figs. 3, 4 and 5). On graphite, the oxygen evolution reaction is least favoured, i.e., it becomes noticeable in the potentiodynamic plot at higher anodic potentials. For instance, in figure 6, the curve for condition 4 (second curve from the top) appears to reach its

limiting current density at about 1.8 V, before water decomposition takes over.

Further tests were carried out with 0.5 M sulfuric acid in the anolyte in order to provide better electrical conductivity and, therefore, a lower cell voltage.

### 4.3. Ferrous sulfate concentration

Experiments performed at 0.5 M and 1 M ferrous sulfate show that the limiting current density ($i_L$) for ferrous ion oxidation increases with ferrous sulfate concentration, which is predicted by Fick's law (eq. 4). However, the $i_L$ increase with ferrous concentration is less than expected, i.e., doubling the concentration does not lead to doubling the limiting current density value. This can be explained as follows: the mass transfer coefficient (k) is not constant, but it depends on temperature, agitation, viscosity and density of the solution. At constant agitation, the diffusion layer thickness ($\delta$) is constant, but an increasing concentration of ferrous sulfate causes an increase in the viscosity of the solution, which, in turn, forces a decrease in the value of the ferrous ion diffusivity (D), mass transfer coefficient and limiting current density. The decrease in the value of k partially offsets the increase in ferrous sulfate concentration.

Cooke (1989) stated that there is a 0.2 M threshold ferrous ion concentration beyond which the limiting current density for $Fe^{2+}/Fe^{3+}$ oxidation increases less steeply than it does at lower concentrations. Values for the mass transfer coefficient of ferrous ion during $Fe^{2+}/Fe^{3+}$ oxidation on platinum (Fig. 2) range from $3.10^{-3}$ m/s (agitation setting = 2; T = 25 °C) to $16.10^{-3}$ m/s (agitation setting = 7; T = 50 °C).

### 4.4. Temperature

The effect of increasing temperature is to increase the oxidation rate, as can be clearly seen in figures 1 to 7 from a comparison between curves at 25 °C and 50 °C. Temperature acts in a similar fashion to ferrous ion concentration, as it also affects the value of the limiting current density. Temperature does so by increasing ion mobilities and diffusivities.

### 4.5. Anodic catalysis

Table IV shows the calculated kinetic parameters for ferrous ion oxidation at conditions 4 and 5, as described in table I. There is a relative error of up to 5 % associated to these parameters, which originates in the fact that they were obtained from experimental curves.

Values for the anodic charge transfer coefficient ($\alpha_a$) are fairly similar for all materials, which indicates that the anodic reaction mechanism does not change by changing the anode composition. This is consistent with other published work[13, 15 and 32].

It is clear, from the potentiodynamic plot (Fig. 7) that ferrous ion oxidation on lead is very slow throughout the studied potential range, hence, the use of a lead anode for this reaction, in the studied conditions, should be ruled out.

For a reaction which takes place under charge transfer or mixed control, the value of its exchange current density ($i_0$) on various electrode materials can be taken as a measure of the catalytic capacities of such materials, i.e. the higher the $i_0$, the better the catalyst. Results in table IV show that, in decreasing order of exchange current densities, the studied materials rank as follows:

Condition 4:

$$i_{0,Pt} > i_{0,Pt/Ti} > i_{0,gr} > i_{0,RuO2/Ti} > i_{0,IrO2/Ti}$$

Condition 5:

$$i_{0,Pt} > i_{0,Pt/Ti} > i_{0,RuO2/Ti} > i_{0,IrO2/Ti} > i_{0,gr}$$

which means that, for the studied reaction in the studied conditions, Pt is a better catalyst than Pt/Ti and the latter is better than the remaining three materials.

The overpotential of the anodic reaction ($\eta_a$) can be taken as a second measure of the catalytic capacity of the studied materials. In this case, the higher the anodic overpotential for $Fe^{2+}/Fe^{3+}$ oxidation on a given anode, the worse its catalytic properties. In table V, the anodic overpotentials were calculated for condition 5 and for three current densities.

In increasing order of anodic overpotential, the anode materials rank as follows:

$$\eta_{a,Pt} < \eta_{a,Pt/Ti} < \eta_{a,RuO2/Ti} < \eta_{a,gr} < \eta_{aIrO2/Ti}$$

From all three rankings and the results in table V, it is possible to conclude that Pt is the best catalyst for the studied reaction and conditions, while the performances of the remaining anode

materials are not widely different. This result is economically relevant, as the cost of Pt/Ti, $RuO_2$/Ti, $IrO_2$/Ti and graphite anodes varies over a wide range; this means that a relatively low cost alternative can be chosen for an industrial application without significant loss of efficiency.

## 5. CONCLUSIONS

- The electrolytic $Fe^{2+}/Fe^{3+}$ oxidation rate in aqueous $FeSO_4 - H_2SO_4$ solutions depends on ferrous ion concentration, electrolyte temperature and degree of agitation. Sulfuric acid concentration does not significantly affect the reaction rate.
- From potentiodynamic experiments, it was shown that, in the studied conditions, the anodic reaction is fastest on Pt and slowest on Pb, which is ruled out as anode material for this reaction. The performances of the remaining anode materials (Pt/Ti, $RuO_2$/Ti, $IrO_2$/Ti and graphite) are satisfactory and not widely different.
- The use of $Fe^{2+}/Fe^{3+}$ as anodic reaction in new copper electrowining cells can be further explored, as these results show that anode materials of relatively low cost can be used without significant loss of efficiency.

## Acknowledgements

This work was funded by the National Committee for Science and Technology (CONICYT, Chile) via FONDECYT project No. 101 0138. Financial help from Barrick and Placer Dome to the Chair of Environmental Studies in Mining, as well as the continued support from the Department of Mining Engineering, Universidad de Chile, are gratefully acknowedged. Thanks are due to Gloria Crisóstomo for her help in the preparation of the present paper.

## List of Symbols

| | |
|---|---|
| c | concentration, mol $L^{-1}$ |
| D | diffusivity, $m^2$ $s^{-1}$ |
| F | Faraday's constant, C $eq^{-1}$ |
| gr | graphite |
| $i_{MC}$ | current density under mixed control, A $m^{-2}$ |
| $i_{CTC}$ | current density under charge transfer control, A $m^{-2}$ |
| $i_{MTC}$ | current density under mass transfer control, A $m^{-2}$ |
| $i_L$ , $i_{L,a}$, $i_{L,c}$ | limiting current density, anodic and cathodic, A $m^{-2}$ |
| $i_0$ , $i_{0,a}$, $i_{0,c}$ | exchange current density, anodic and cathodic, A $m^{-2}$ |
| k | mass transfer coefficient, m $s^{-1}$ |
| R | Gas constant, J $mol^{-1}$ $K^{-1}$ |
| t | time of operation, s |
| T | temperature, K |
| $z$ | charge number |
| $\alpha_a$, $\alpha_c$ | anodic, cathodic charge transfer coefficients |
| $\delta$ | thickness of the diffusion layer, m |
| $\eta$, $\eta_a$, $\eta_c$ | overpotential, anodic and cathodic, V |

## REFERENCES

[1] L. CIFUENTES, R. GLASNER, G. CRISÓSTOMO, J.M. CASAS and J. SIMPSON, *Meeting Abstracts*, 201st Meeting of the Electrochemical Society, Philadelphia, 2002, ECS, New York, USA, Abstract No.1122.
[2] R. KAMMEL, JOM 10 (1981) 45-48.
[3] R. KAMMEL, *Hydrometallurgical Process Fundamentals*, R. Bautista (Ed.), Plenum Press, New York, USA, 1982, pp. 617-648.
[4] R. KAMMEL, *Proc. 3rd Internat. Symp. on Hydrometallurgy*, New York, 1982, AIME, New York, USA, 647-657.
[5] W.C. COOPER, *J. Appl. Electrochem.* 15(1985) 789-805.
[6] D.W. DEW, *Hydrometallurgy* 14 (1985) 331-349.
[7] D.W. DEW, *Hydrometallurgy* 14 (1985) 351-367.
[8] C.K. GUPTA and T.K. MUKHERJEE, *Hydrometallurgy in Extraction Processes*, CRC Press, Boca Raton, USA, 1990, pp. 228-242.
[9] F. COEURET, *Introducción a la ingeniería electroquímica*, Ed. Reverté, Barcelona, Spain, 1992, pp. 225-248.
[10] K.P. GOPALA, *Hydrometallurgy* 31 (1992) 243-255.
[11] T. SUBBAIAH, S.C. DAS and R.P. DAS, *Hydrometallurgy* 33 (1993) 153-163.
[12] F.C. WALSH, *A first course in electrochemical engineering*, The Electrochemical Consultancy, Romsey, UK, 1993, p. 112.
[13] A.V. COOKE, J.P. CHILTON and D.J. FRAY, *Trans. Instn. Min. Metall.* (Sec. C: Mineral Processing Extr. Metall.) 98 (1989) 123-131.
[14] S.P. SANDOVAL, W.J. DOLINAR, J.W. LANGHANS and K.P.V. LEI, *Proc. COPPER '95 Int. Conf.*, Vol. 3, Toronto, 1995, W.C. Cooper (Ed.), The Metallurgical Soc. of CIM, Toronto, Canada, 1995, pp. 423-35.
[15] V. JIRICNY, A. ROY and J.W. EVANS, Proc. *COPPER'99 Int. Conf.*, Vol.3, Phoenix, 1999, J. Dutrizac (Ed.), TMS, Phoenix, USA, 1999, pp. 629-642.

[16] G.H. CHEN, X.M. CHEN and P.L. YUE, *J. Phys. Chem. B* 106 (2002) 4364-4369.

[17] S.C. DAS and P.G. KRISHNA, Int. *J. Mineral Proc.* (1996) 91-105.

[18] J.C. LEE, H.B. DARUS and S.H. LANGER, *J. Appl. Electrochem.* 23 (1993) 745-752.

[19] P.F. MARCONI, V. MEUMER and N. VATISTAS, *J. Appl. Electrochem.* 26 (1996) 693-701.

[20] S.R. RAO, J.A. FINCH and N. KUYUCAK, *Miner. Eng.* 8 (1995) 905-911.

[21] M.R. RONNHOLM, J. WARNA, T. SALMI, I. TURUNEN and M. LUOMA, *Chem. Eng. Sci.* 54 (1999) 4223-4232.

[22] M.R. RONNHOLM, J. WARNA, T. SALMI, I. TURUNEN and M. LUOMA, *Ind. Eng. Chem. Res.* 38 (1999) 2607-2614.

[23] S.B. HALL and G.A. WRIGHT, *Corros. Sci.* 31 (1990) 709-714.

[24] R.R. MOSKALYK, A. ALFANTAZI and A.S. TOMBALAKIAN, *Miner. Eng.* 12 (1999) 65-73.

[25] M. UEDA, A. WATANABE and T. KAMEYAMA, *J. Appl. Electrochem.* 25 (1995) 817-822.

[26] G. CIFUENTES and L. CIFUENTES, *Corros. Sci.* 40 (1998) 225-34.

[27] G. CIFUENTES, L. CIFUENTES, R. KAMMEL, J. TORREALBA and A. CAMPI, *Z. Metallkunde* 89 (1998) 363-367.

[28] G. CIFUENTES, J. SIMPSON, L. CIFUENTES and G. CRISÓSTOMO, *Proc. COPPER '99 Int. Conf.*, Vol.3, Phoenix, 1999, J. Dutrizac (Ed.), TMS, Phoenix, USA, 1999, p. 585.

[29] G. CIFUENTES, J. TORREALBA, L. CIFUENTES and R. KAMMEL, *Z. Metallkunde* 91 (2000) 6.

[30] L. CIFUENTES, G. CRISÓSTOMO, J.P. IBÁÑEZ, J.M. CASAS, F. ALVAREZ and G. CIFUENTES, *J. Membr. Sci.* 207 (2002) 1-16.

[31] J.O'M. BOCKRIS, A.K. N. REDDY and A.M. GAMBOA-ALDECO, *Modern Electrochemistry*, 2nd Ed., Vol. 2A, Plenum, 1999, p. 1250.

[32] Z. NAGY, L.A. CURTISS and N. C. HUNG, *J. Electroanal. Chem.* 325 (1992) 313-324.